

2010

# Spontaneous transition to superrotation in warm climates simulated by CAM3

Rodrigo Caballero  
*University College Dublin*

Matthew Huber  
*Purdue, huberm@purdue.edu*

Follow this and additional works at: <http://docs.lib.purdue.edu/easpubs>

---

## Repository Citation

Caballero, Rodrigo and Huber, Matthew, "Spontaneous transition to superrotation in warm climates simulated by CAM3" (2010).  
*Department of Earth, Atmospheric, and Planetary Sciences Faculty Publications*. Paper 32.  
<http://dx.doi.org/10.1029/2010GL043468>

This document has been made available through Purdue e-Pubs, a service of the Purdue University Libraries. Please contact [epubs@purdue.edu](mailto:epubs@purdue.edu) for additional information.



## Spontaneous transition to superrotation in warm climates simulated by CAM3

Rodrigo Caballero<sup>1</sup> and Matthew Huber<sup>2</sup>

Received 30 March 2010; revised 1 May 2010; accepted 10 May 2010; published 5 June 2010.

[1] Recent paleoclimate proxy reconstructions show that tropical surface temperatures may have been as high as 35°–40°C in the Early Cenozoic. Here, we study the tropical atmospheric circulation's response to temperatures in this range using a full-complexity atmospheric general circulation model (AGCM). We find that when equatorial surface temperatures exceed ~33°C, the model undergoes a transition to equatorial superrotation, a state with strong annual- and zonal-mean westerlies on the equator. The transition is driven by zonal momentum convergence due to large-amplitude transient eddies on the equator. These eddies have a structure similar to the observed Madden-Julian Oscillation (MJO). The model's MJO variability is weaker than observed when simulating the modern climate but increases sharply with temperature, coming to dominate the tropical variability and mean state of the warmest climates. **Citation:** Caballero, R., and M. Huber (2010), Spontaneous transition to superrotation in warm climates simulated by CAM3, *Geophys. Res. Lett.*, 37, L11701, doi:10.1029/2010GL043468.

### 1. Introduction

[2] Little is known about tropical dynamics at temperatures much warmer than today. Studies of altered climates generally focus on the range of warming expected over the next century, typically a few degrees. Some climates of the deep past—in the Cretaceous and Eocene in particular—have long been known for extreme extratropical warmth, but it was generally thought until recently that tropical temperatures were close to modern (as summarized by *Huber and Sloan* [2000]). This view has been challenged by recent studies [*Pearson et al.*, 2007; *Huber*, 2008] suggesting tropical sea surface temperature (SST) may have been as high as 35°C during the Early Eocene and perhaps 5°C higher during 'hyperthermal' events such as the Paleocene-Eocene Thermal Maximum [*Zachos et al.*, 2003]. These results warrant much closer attention to tropical dynamics under very hot conditions.

[3] Here, we study the response of the tropical atmospheric circulation to extreme warmth using a comprehensive atmospheric general circulation model (AGCM). We focus on changes in the zonal momentum balance and the possibility of equatorial superrotation—a state of the atmospheric general circulation with mean westerlies on the equator (I. M.

Held, Equatorial superrotation in Earth-like atmospheric models, 1999, available online at <http://www.gfdl.gov>).

[4] Observational studies of the modern climate show a close balance between momentum convergence onto the equator by tropical eddies and momentum divergence by the zonal-mean circulation, particularly the cross-equatorial solstitial Hadley cells [*Lee*, 1999; *Dima et al.*, 2005]. As a result, equatorial zonal-mean winds near the tropopause are close to zero in the annual mean. In a warmer climate, the balance could tip in favor of superrotation if tropical eddy activity increases and/or the Hadley cells weaken. A number of model studies have in fact reported modestly increased equatorial angular momentum in response to global-mean warming of a few degrees [*Lee*, 1999; *Huang et al.*, 2001]. *Lee* [1999] specifically attributed this change to increased MJO activity. Cloud-resolving model studies [e.g., *Grabowski*, 2003] and theoretical work [*Moncrieff*, 2004; *Biello et al.*, 2007] suggests that the MJO naturally favors superrotation because of the intrinsic meridional and vertical tilts in the MJO's planetary scale structure. Based on this evidence, *Tziperman and Farrell* [2009] strongly advocate the idea that superrotation could play an important role in past and future warm climates.

[5] Our aim here is to document—for the first time, so far as we are aware—a spontaneous transition to strong superrotation taking place in a state-of-the-art AGCM. By 'spontaneous' we mean that the transition occurs naturally as part of the model's response to increasing greenhouse forcing, without the addition of an ad hoc equatorial heating perturbation as in previous work [*Battisti and Ovens*, 1995; *Hoskins et al.*, 1999; *Inatsu et al.*, 2002; *Kraucunas and Hartmann*, 2005]. The model experiments and results are summarized in section 2, the eddy structure is examined in section 3 and the results are discussed in section 4.

### 2. Model Experiments and Results

[6] We use the National Center for Atmospheric Research (NCAR) Community Atmosphere Model version 3.1 (CAM3) [*Collins et al.*, 2006]. To explore the robustness of the transition, we employ 3 different model configurations: the default, modern configuration; a configuration with Early Eocene geography, land surface cover and no ice sheets [*Liu et al.*, 2009; *Williams et al.*, 2009]; and an aquaplanet configuration. In all cases, the model is coupled to a slab ocean with prescribed ocean heat transport (OHT). For each configuration, we perform a sequence of simulations with successive doublings of atmospheric CO<sub>2</sub> concentration, starting from a preindustrial value (280 ppm) and reaching 5 doublings (8960 ppm) for the Eocene and aquaplanet cases, and 6 doublings (17920 ppm) for the modern case. The simulations are all conducted at T42

<sup>1</sup>Meteorology and Climate Centre, School of Mathematical Sciences, University College Dublin, Dublin, Ireland.

<sup>2</sup>Earth and Atmospheric Sciences, Purdue University, West Lafayette, Indiana, USA.

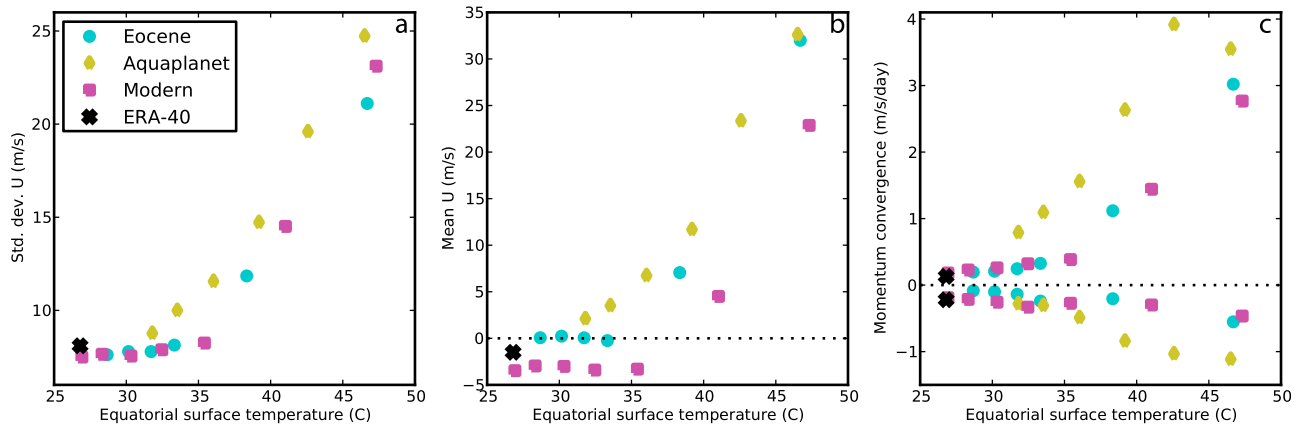


**Figure 1.** Summary results from the model runs as a function of equatorial-mean SST ( $5^{\circ}\text{S}$ – $5^{\circ}\text{N}$ ). Large crosses indicate corresponding results from the ECMWF ERA-40 reanalysis product. All quantities plotted here are annual long-term averages around the equatorial tropopause ( $5^{\circ}\text{S}$ – $5^{\circ}\text{N}$ , 50–150 hPa). (a) Standard deviation of transient-eddy zonal wind, a gross measure equatorial eddy activity. (b) Zonal-mean zonal wind. (c) Zonal momentum convergence by transient eddies (positive values) and by the zonal-mean circulation (negative values).

spectral resolution ( $\sim 2.5^{\circ} \times 2.5^{\circ}$ ). A 10 minute time step is used to ensure numerical stability in all cases. OHT is held fixed at the observationally-derived present-day value in the modern runs. The aquaplanet simulations uses the same OHT but rendered zonally and hemispherically symmetric. The Eocene is simulated using OHT and mixed layer depth derived from a corresponding set of equilibrated fully-coupled model (CCSM3) Eocene simulations [Liu *et al.*, 2009] using the same  $\text{CO}_2$ -doubling sequence as the slab-ocean runs.

[7] Figure 1 presents an overview of results. In the simulations with low  $\text{CO}_2$  and modern or Eocene boundary conditions, equatorial SSTs are near modern values ( $\sim 27^{\circ}\text{C}$ ) and results agree reasonably well with observations, though it is clear that this model underestimates observed modern tropical eddy variability, as noted in previous work [Collins *et al.*, 2006]. There is little change in the results as SST increases up to  $\sim 33^{\circ}\text{C}$ . Beyond this point, however, transient eddy activity becomes strongly sensitive to SST, increasing roughly 4-fold as SST rises to  $47^{\circ}$  (Figure 1a).

Over the same range, tropopause westerly winds accelerate from near-zero to about  $33 \text{ m s}^{-1}$  (Figure 1b). This change in the winds is due to increased momentum convergence by the transient eddies (Figure 1c). Momentum divergence by the zonal-mean circulation also increases somewhat with SST, but much less than eddy momentum convergence; as result, the balance tips in favour of strong mean westerlies.

[8] Figure 2 compares climatological cross sections from the coldest and warmest aquaplanet runs. The colder run (Figure 2a) shows the conventional picture with near-zero equatorial winds, peak eddy activity in the midlatitude storm tracks and Eliassen-Palm fluxes directed upwards and equatorwards. The warm case is dramatically different, with much weaker eddy activity in midlatitudes—consistent with prior work [Caballero and Langen, 2005; O’Gorman and Schneider, 2008]—and peak activity at the equatorial tropopause (which has risen to around 70 hPa). Strong poleward Eliassen-Palm fluxes emanate from this region, indicating zonal momentum convergence which drives strong equatorial superrotation. At intermediate temperatures, the patterns

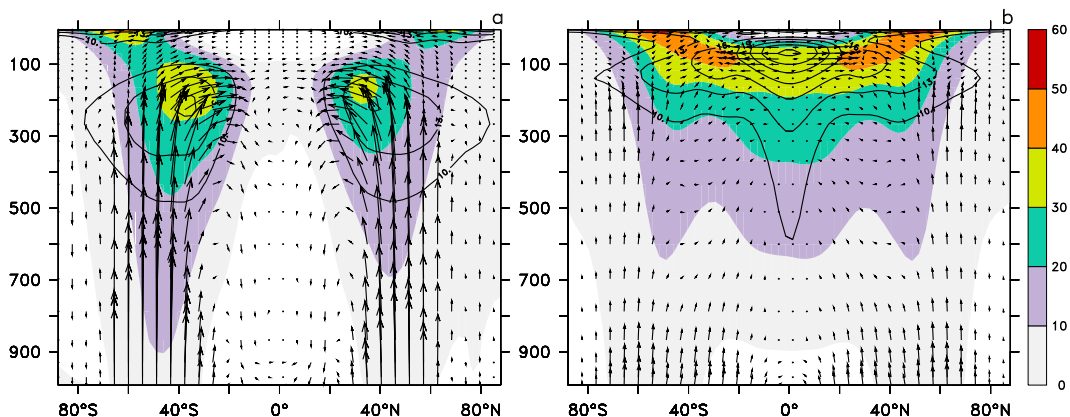


**Figure 2.** Zonal-mean climatologies of the aquaplanet runs with (a) 280 ppm and (b) 8960 ppm (5 doublings) atmospheric  $\text{CO}_2$  concentration. Shading shows zonal wind ( $\text{m s}^{-1}$ ), contours show standard deviation of transient-eddy zonal wind ( $\text{m s}^{-1}$ ), and vectors show the Eliassen-Palm flux, plotted as in the work of Edmon *et al.* [1980].

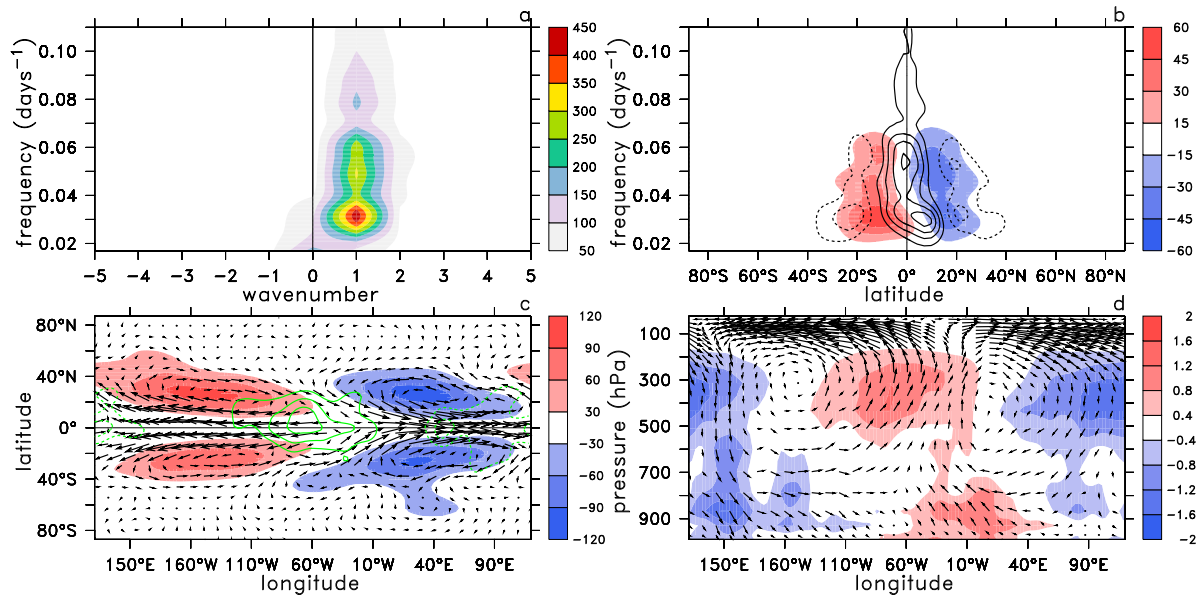


**Figure 3.** (a) Space-time spectrum of zonal wind at the equatorial tropopause (70 hPa, 5°S–5°N average) in the 8960 ppm CO<sub>2</sub> aquaplanet run. Positive wavenumbers imply eastward propagation. The spectrum is smoothed along the frequency axis with a Gaussian filter of half-width 0.01 days<sup>-1</sup>. (b) Frequency spectrum of eddy momentum flux (shading) and eddy momentum flux convergence (contours) filtered to retain only zonal wavenumber 1. EOF analysis of 70 hPa zonal wind in the 8960 ppm CO<sub>2</sub> aquaplanet run. Plots show regression of the standardised principal component associated with the leading EOF mode onto (c) 70 hPa geopotential height (shading, c.i. 30 m), 70 hPa horizontal wind (vectors, longest is about 15 m s<sup>-1</sup>), and precipitation (green contours at 0.5 mm day<sup>-1</sup> intervals) and (d) equatorial specific humidity (shading, c.i. 2 g kg<sup>-1</sup>) and vertical-zonal wind (vectors, pressure velocity has sign reversed and is scaled by 200 for display purposes).

are intermediate between the extremes displayed in Figure 2. Qualitatively similar changes take place in the modern and Eocene-configuration runs.

### 3. Nature of Equatorial Eddy Activity

[9] We now examine the spatio-temporal characteristics of the tropical eddy activity, focusing on the warmest aquaplanet run (Figure 2b). Space-time spectral analysis, Figure 3, reveals that zonal wind eddy variance at the equatorial tropopause is dominated by planetary-scale (zonal wavenumber 1) waves propagating eastward with periods between about 15 and 30 days (Figure 3a). These waves are responsible for the momentum convergence required to drive superrotation (Figure 3b).

[10] To investigate the spatial structure of the waves, we use empirical orthogonal function (EOF) analysis of the zonal wind at the tropopause level between 30°S and 30°N. Given the dominance of zonally propagating waves, EOF decomposition gives two leading modes with the same explained variance and structure, but shifted 90° out of phase in the zonal direction. The two leading modes each explain about 20% of the variance, and are very well separated from the third mode, that explains 6% of the variance. The principal components (PCs) associated with these two modes have maximum lag correlation of 0.6 at about 4.5 day lag; this implies a period of 18 days, in agreement with the spectral results above. We take the PC associated with one of the leading modes, and regress it onto wind, geopotential

height, precipitation and humidity to determine the spatial structure of these fields associated with the leading mode.

[11] At the tropopause (Figure 3c), the leading mode exhibits strong wavenumber-1 zonal wind anomalies with peak amplitude on the equator. A positive precipitation anomaly (indicative of a tropospheric latent heating anomaly) appears in the region of easterly flow. A prominent quadrupole structure is apparent in the height field, with anticyclones flanking the equator upstream of the heating perturbation and cyclones downstream. These structures can be interpreted as Matsuno-Gill-type Rossby-Kelvin wave couplets [Seo and Kim, 2003; Matthews *et al.*, 2004]. The meridional tilt of these gyres is such as to produce zonal momentum convergence onto the equator. A vertical cross-section along the equator (Figure 3d) shows that the tropopause anomalies extend downward throughout the troposphere, taking the form of twin overturning circulations with low-level return flow maximising around the 800 hPa level. Low-level humidity anomalies appear roughly in quadrature with the heating.

[12] All these features are very strongly reminiscent of the observed modern-day MJO (see Zhang [2005] for a review). The 15–30 day timescale is short compared with the observed MJO's timescale of 30–100 days, however. This short timescale is also apparent in modern climate simulations using this model [Collins *et al.* 2006, Figure 10]. This might suggest that intraseasonal variability in the hot climates shares the same fundamental nature as that in colder climates simulated by the model; on the other hand, the hot-climate eddies could be closer to a true, slow-moving MJO

mode which is then Doppler shifted by the strong superrotation winds. Further work is necessary to clarify this issue.

#### 4. Discussion and Implications

[13] We find that CAM3 exhibits a spontaneous transition to strong superrotation when equatorial SSTs exceed about 33°C. The transition is driven by the onset of large-amplitude MJO-like intraseasonal variability in which upper-tropospheric Rossby gyres induce strong zonal momentum convergence onto the equator.

[14] The transition to superrotation found here is rather gradual, with equatorial westerlies increasing smoothly with eddy variability. This is different to the abrupt transition found in previous work using 2-level models [Suarez and Duffy, 1992; Saravanan, 1993]. There is no seasonal cycle in these simplified models, and momentum convergence on the equator due to tropical eddies is balanced by momentum divergence due to extratropical eddy absorption at critical lines near the equator. As tropical eddy forcing increases, equatorial winds gradually accelerate until the critical lines disappear, allowing the zonal-mean wind to accelerate discontinuously into the strongly superrotating state. In observations [Lee, 1999] and in the AGCM, on the other hand, equatorial deceleration is due mainly to negative vorticity flux by the cross-equatorial Hadley cells. As Figure 1c shows, this flux actually increases somewhat as superrotation sets in. Hence the more linear response found here: superrotation increases roughly proportionally to tropical eddy amplitude.

[15] A transition to superrotation could feed back on climate in critical ways. Strong vertical wind shear in the tropics should affect convective organization on all scales, and in particular could inhibit the formation of tropical cyclones. It could also change the index of refraction of the tropical tropopause, affecting stratospheric circulation [Korty and Emanuel, 2007]. The disruption to the atmospheric zonal momentum balance and consequent reorganization of surface winds could also have important consequences for the global wind-driven ocean circulation. It has been suggested that superrotation would be accompanied by weakened easterly or even westerly surface stress along the equator, which could tip the Pacific basin into a ‘permanent El Niño’ state [Pierrehumbert, 2000; Tziperman and Farrell, 2009]. The slab-ocean configuration used here precludes coupled ocean-atmosphere variability, but we note that zonal-mean zonal wind stress along the equator drops by roughly 30% between the coldest and warmest runs in both modern and Eocene configurations.

[16] The outstanding question, of course, is what causes the tropical intraseasonal variability to amplify once temperatures exceed ~33°C. This question is difficult to answer given the current absence of a complete and generally accepted theory for the MJO, despite consistent progress in that direction [Zhang, 2005; Sobel et al., 2008; Majda and Stechmann, 2009]. It seems likely that the amplification mechanism involves radiative-convective and surface flux feedbacks, and thus hinges on the model’s sub-gridscale parameterizations. The parameterizations were developed and tuned for the modern climate, so caution should be exercised in interpreting these results. However, analysis of the bulk properties of tropical convection in the model

[Williams et al., 2009] strongly suggest that the model is behaving as expected from quasi-equilibrium convection theory even in very warm climates. Furthermore, as noted in section 2, the version of CAM3 used here produces a rather weak MJO under modern conditions [Collins et al., 2006], so there is no obvious reason to suspect that the model is intrinsically biased towards high-amplitude MJO variability.

[17] More work is needed to better understand the nature, realism and robustness of our results. Further studies using a range of conventional and superparameterized AGCMs and full cloud-resolving models would be particularly valuable, and we hope that this paper will serve to stimulate research in this direction within the modelling community. If the route to superrotation explored here turns out to be robust and realistic, the MJO would emerge as a dominant player in past and possibly future climate change.

[18] **Acknowledgments.** We are grateful to Cecilia Bitz for the slab-ocean aquaplanet configuration of CAM3 and to Eli Tziperman and an anonymous reviewer for their comments. R.C. is funded by SFI grant GEOF252. M.H. is funded by the U.S. NSF grant 0902844. This is PCCRC contribution 1013.

#### References

- Battisti, D., and D. Ovens (1995), The dependence of the low-level equatorial easterly jet on Hadley and Walker circulations, *J. Atmos. Sci.*, *52*, 3911–3931.
- Biello, J., A. Majda, and M. Moncrieff (2007), Meridional momentum flux and superrotation in the multiscale IPESD MJO model, *J. Atmos. Sci.*, *64*, 1636–1651.
- Caballero, R., and P. Langen (2005), The dynamic range of poleward energy transport in an atmospheric general circulation model, *Geophys. Res. Lett.*, *32*, L02705, doi:10.1029/2004GL021581.
- Collins, W., et al. (2006), The formulation and atmospheric simulation of the Community Atmosphere Model: CAM3, *J. Clim.*, *19*, 2144–2161.
- Dima, I. M., J. M. Wallace, and I. Kraucunas (2005), Tropical zonal momentum balance in the NCEP reanalyses, *J. Atmos. Sci.*, *62*, 2499–2513.
- Edmon, H. J., B. J. Hoskins, and M. E. McIntyre (1980), Eliassen-Palm cross sections for the troposphere, *J. Atmos. Sci.*, *37*, 2600–2616.
- Grabowski, W. (2003), MJO-like coherent structures: Sensitivity simulations using the cloud-resolving convection parameterization (CRCP), *J. Atmos. Sci.*, *60*, 847–864.
- Hoskins, B., R. Neale, M. Rodwell, and G. Yang (1999), Aspects of the large-scale tropical atmospheric circulation, *Tellus A*, *51*, 33–44.
- Huang, H., K. Weickmann, and C. Hsu (2001), Trend in atmospheric angular momentum in a transient climate change simulation with greenhouse gas and aerosol forcing, *J. Clim.*, *14*, 1525–1534.
- Huber, M. (2008), A hotter greenhouse, *Science*, *321*, 353–354.
- Huber, M., and L. Sloan (2000), Climatic responses to tropical sea surface temperature changes on a “greenhouse” Earth, *Paleoceanography*, *15*, 443–450.
- Inatsu, M., H. Mukougawa, and S. Xie (2002), Stationary eddy response to surface boundary forcing: Idealized GCM experiments, *J. Atmos. Sci.*, *59*, 1898–1915.
- Korty, R., and K. Emanuel (2007), The dynamic response of the winter stratosphere to an equable climate surface temperature gradient, *J. Clim.*, *20*, 5213–5228.
- Kraucunas, I., and D. Hartmann (2005), Equatorial superrotation and the factors controlling the zonal-mean zonal winds in the tropical upper troposphere, *J. Atmos. Sci.*, *62*, 371–389.
- Lee, S. (1999), Why are the climatological zonal winds easterly in the equatorial upper troposphere?, *J. Atmos. Sci.*, *56*, 1353–1363.
- Liu, Z., M. Pagani, D. Zinniker, R. DeConto, M. Huber, H. Brinkhuis, S. Shah, R. Leckie, and A. Pearson (2009), Global cooling during the Eocene-Oligocene climate transition, *Science*, *323*, 1187–1190.
- Majda, A., and S. Stechmann (2009), The skeleton of tropical intraseasonal oscillations, *Proc. Natl. Acad. Sci. U. S. A.*, *106*, 8417–8422.
- Matthews, A., B. Hoskins, and M. Masutani (2004), The global response to tropical heating in the Madden-Julian oscillation during the northern winter, *Q. J. R. Meteorol. Soc.*, *130*, 1991–2012.
- Moncrieff, M. (2004), Analytic representation of the large-scale organization of tropical convection, *J. Atmos. Sci.*, *61*, 1521–1538.

- O’Gorman, P., and T. Schneider (2008), Energy of midlatitude transient eddies in idealized simulations of changed climates, *J. Clim.*, *21*, 5797–5806.
- Pearson, P., B. Van Dongen, C. Nicholas, R. Pancost, S. Schouten, J. Singano, and B. Wade (2007), Stable warm tropical climate through the Eocene epoch, *Geology*, *35*, 211–214.
- Pierrehumbert, R. T. (2000), Climate change and the tropical Pacific: The sleeping dragon wakes, *Proc. Natl. Acad. Sci. U. S. A.*, *97*, 1355–1358.
- Saravanan, R. (1993), Equatorial superrotation and maintenance of the general circulation in two-level models, *J. Atmos. Sci.*, *50*, 1211–1227.
- Seo, K., and K. Kim (2003), Propagation and initiation mechanisms of the Madden-Julian oscillation, *J. Geophys. Res.*, *108*(D13), 4384, doi:10.1029/2002JD002876.
- Sobel, A., E. Maloney, G. Bellon, and D. Frierson (2008), The role of surface heat fluxes in tropical intraseasonal oscillations, *Nat. Geosci.*, *1*, 653–657.
- Suarez, M., and D. Duffy (1992), Terrestrial superrotation: A bifurcation of the general circulation, *J. Atmos. Sci.*, *49*, 1541–1554.
- Tziperman, E., and B. Farrell (2009), Pliocene equatorial temperature: Lessons from atmospheric superrotation, *Paleoceanography*, *24*, PA1101, doi:10.1029/2008PA001652.
- Williams, I., R. Pierrehumbert, and M. Huber (2009), Global warming, convective threshold and false thermostats, *Geophys. Res. Lett.*, *36*, L21805, doi:10.1029/2009GL039849.
- Zachos, J., M. Wara, S. Bohaty, M. Delaney, M. Petrizzo, A. Brill, T. Bralower, and I. Premoli-Silva (2003), A transient rise in tropical sea surface temperature during the Paleocene-Eocene thermal maximum, *Science*, *302*, 1551–1554.
- Zhang, C. (2005), Madden-Julian oscillation, *Rev. Geophys.*, *43*, RG2003, doi:10.1029/2004RG000158.

---

R. Caballero, Meteorology and Climate Centre, School of Mathematical Sciences, University College Dublin, Belfield, Dublin 4, Ireland. (rodrigo.caballero@ucd.ie)

M. Huber, Department of Earth and Atmospheric Sciences, Purdue University, 550 Stadium Mall Dr., West Lafayette, IN 47907, USA. (huberm@purdue.edu)